Available online at www.sciencedirect.com
SCIENCE DIRECT
Journal of Sound and Vibration 297 (2006) 420–431
JOURNAL OF SOUND AND VIBRATION
www.elsevier.com/locate/jsvi

Short communication

Diagnosis of a portal frame using advanced signal processing of laser vibrometer data

Joseph Morlier[a,b,*], Frédéric Bos[a], Patrick Castéra[a]

[a]*Laboratoire de Rhéologie du Bois de Bordeaux, Domaine de l'Hermitage, 69 route d'Arcachon, 33612 Cestas Gazinet, France*
[b]*XYLOMECA, 41 rue Michel de Montaigne, 24700 Moulin Neuf, France*

Received 26 April 2005; received in revised form 20 March 2006; accepted 30 March 2006
Available online 8 June 2006

Abstract

This paper introduces an original, non-destructive diagnosis tool using modal data only. Our objective is twofold: to identify damage in structural elements (beams) and to establish a classification of the connections between elements using no a priori information except the modal data. This paper introduces enhanced wavelet analysis as a tool for damage detection based on mode shape data, using an analytical mode shape fit as the undamaged state. Then we demonstrate that damage severity can be identified using a supervised neural networks approach. To supplement the local diagnosis, boundary conditions are characterised using spatial frequency. Finally, a damaged beam of a wooden portal is analysed using a high-resolution mode shape acquired with a laser Doppler vibrometer. The experimental results confirm the accuracy of the method for detecting damages and classifying boundary conditions.

1. Introduction

Over the past 20 years, detecting damage in a structure from the changes in its dynamic parameters has received considerable attention from aerospace, mechanical and civil engineering communities. Several approaches of structural health monitoring (SHM) based on vibration techniques have demonstrated their capabilities of detecting defects in structures [1]. The basis of these damage detection methods is that modifications in the properties of a structure will alter its dynamic characteristics. A first approach consists in using modal analysis to measure the natural frequencies of a structure, which can provide useful indications as to the existence of damage zones. However, this simple and fast method has some limitations in locating and quantifying damage zones [2]. To overcome these difficulties, many researchers [3,4,16] have focused on characterising the structural mode shapes, which contain spatial information and appear to be more sensitive to the presence of damage zones than natural frequencies. In this approach accuracy of damage detection depends on the quality of both experimental measurements and signal processing. Particularly, the quality of an approach of SHM using experimental mode shape analysis (especially for small damages detection) is always dependent on the reliability and accuracy of sensors and also on the experimental sampling [8]. For this

*Corresponding author. Tel.: +33557122820; fax: +33556680713.
E-mail address: jmorlier@lrbb.u-bordeaux.fr (J. Morlier).

0022-460X/$ - see front matter © 2006 Elsevier Ltd. All rights reserved.
doi:10.1016/j.jsv.2006.03.044

reason, original studies have been developed using a laser Doppler vibrometer (LDV) [5] or video analysis [6,7]. Otherwise signal processing tools have recently been introduced such as continuous wavelet transform (CWT) [9] in order to detect and identify damage using mode shape data [3,4,10–12].

In order to obtain a complete diagnosis of a structure, boundary conditions (BCs) must also be analysed. This work has been recently introduced, from a theoretical point, of view by Olgac and Jalili [13] which have developed a general analytical formula to identify the BCs on a flexible beam. Practically Pai et al. [14] have successfully identified the boundary effects in beams using spectral element analysis and LDV mode shape data.

The main objective of this paper is to present a complete approach of structural diagnosis, carried out on a simple structure such as a wooden portal frame, and based on the analysis of the local dynamic behaviour of each constitutive element of the structure. The first chapter introduces the link between the structural dynamic behaviour of beams and signal processing of mode shape in order to produce damage identification. Then we present an advanced method which uses the CWT to compute the wavelet singularity map (WSM) for locating singularities on mode shape data. Numerical models are used to validate the method and also to build a large simulated database in order to identify real damage by means of a neural network classification. One of the advantages of this method is that it does not require any a priori information and also it informs about two types of damage assessment: structural and joint. Moreover the extracted features (damage location and extent, BCs class) could be used, for example, to build a posteriori a finite element model, making possible an adapted monitoring of the structure. As an application our method has been validated on a wooden portal frame using a scanning LDV apparatus.

2. Theoretical background

2.1. Damaged beam dynamic behaviour

Classically, the equation used to represent a uniform (undamaged) beam under free vibration can be written as follows:

$$\rho S \frac{\partial^2}{\partial t^2} v(x,t) + EI \frac{\partial^4}{\partial x^4} v(x,t) = 0, \tag{1}$$

where x is the longitudinal coordinate, v is a transversal displacement of the beam in y direction (which is perpendicular to x), t is time, E is the Young's modulus, S is the cross-section area, I is the planar moment of inertia of the cross section, L is the length and ρ is the density of the beam.

Assuming that bending stiffness is independent of time and that the steady-state vibration has a harmonic form, we get:

$$\frac{\mathrm{d}^4 Y(x)}{\mathrm{d}x^4} - \lambda^4 Y(x) = 0. \tag{2}$$

Using separated variables and solving the differential equation, we can express the mode shape as

$$Y_i(x) = A_{1i}\ \cosh(\lambda_i x) + A_{2i}\ \sinh(\lambda_i x) + A_{3i}\ \cos(\lambda_i x) + A_{4i}\ \sin(\lambda_i x), \tag{3}$$

where the spatial frequency of the ith mode is defined as $\lambda_i^2 = \omega_i \sqrt{m/EI}$ with $i = 1 \ldots n$.

The mode shape describes the structure's motion when it is vibrating at a particular frequency.

For a rectangular beam, a simple way to simulate a damage zone consists in introducing a local variation of bending rigidity EI. According to the notation of Fig. 1, for a homogeneous given material a crack zone is defined for an element of width w by the depth ratio c/h. Thus, the inertia reduction factor $\mathrm{d}I$ is defined as

$$\mathrm{d}I = \tilde{I}/I \ \text{ with } \ I = (bh^3)/12 \ \text{ and } \ \tilde{I} = (bc^3)/12. \tag{4}$$

This definition of a damage zone is easily transposable for both simulations and experiments. In these conditions the dynamic response of a beam depends both on depth and position of the crack and on BCs. Olgac [13] has examined the case of an undamaged beam with parametric BCs as depicted in Fig. 1. The

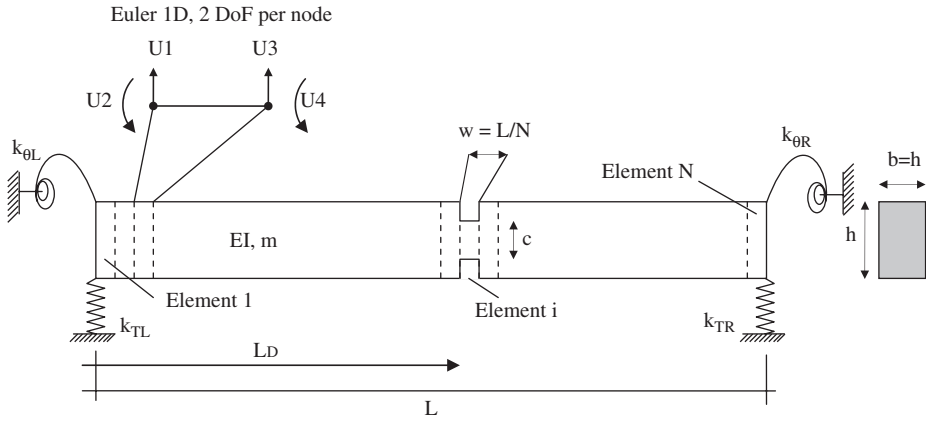

Fig. 1. Simulated damaged beam with elastic spring supports to simulate non-perfect boundary conditions: dimensions and notations.

partially fixed–fixed beam problem has been already studied [15] and our previous work [10] highlighted spatial frequency as a tool to exhibit connection behaviour (perfect or semi-rigid).

2.2. Wavelet transform as a tool for identifying singularities

The principle of SHM using modal data is based on local analysis of regularity of mode shapes. To reach this goal the signal should be analysed by functions which are localised in both time and frequency in order to represent the frequency behaviour of a signal locally in time. A performing tool classically used for this kind of problem is wavelet transform.

The wavelet is an oscillary function $\psi \in L^2(R)$ having a zero average and a finite length (compact support). The real or complex-value function $\psi(x)$ is used to generate a family of wavelets $\psi_{u,s}(x)$, defined as

$$\psi_{u,s}(x) = \frac{1}{\sqrt{s}}\psi\left(\frac{x-u}{s}\right), \tag{5}$$

where real numbers s and u denote the scale and translation parameters, respectively.

For a spatial one-dimensional signal $f(x)$ the wavelet transform can be obtained by integrating the product of the signal function and the complex conjugate $\psi^*(x)$ of the wavelet function.

Considering the mode shape of the beam as a one-dimensional signal $f(x)$, where the variable x is space, the CWT can be defined as

$$Wf(u,s) = \int_{-\infty}^{+\infty} f(x)\frac{1}{\sqrt{s}}\psi^*\left(\frac{x-u}{s}\right)\mathrm{d}x. \tag{6}$$

If the signal contains a spectral component corresponding to the current value of s, the product of the wavelet with the signal gives a relatively large value of the wavelet coefficient $Wf(u,s)$ at the location u where this spectral component exists.

This scalogram is a joint time-scale representation of a one-dimensional signal. This means that the spectral information of the signal is described at all observation scales and at all times. As the scales are related to the frequency of the wavelet, the scalogram provides coarse features of the signal $f(x)$ for large wavelets (high scales, low frequencies) and finer details of the signal for small wavelets (fine scales).

An important characteristic of a wavelet is its number of vanishing moments n, which are used to analyse the local regularity of a signal:

$$\int_{-\infty}^{+\infty} t^k\psi(x)\,\mathrm{d}x = 0 \quad \text{for} \quad 0 \leqslant k \leqslant n. \tag{7}$$

For example, a wavelet with only one vanishing moment is orthogonal to a linear function and can be used to measure the regularity of the function between 0 and 1. A high n number increases the quality of the analysis

but also increases the number of computations as the support length of the wavelet increases ($2n-1$). Mallat and Hwang [9] showed that the maxima of the modulus of the CWT were related to isolated singularities of the signal. A practical way to characterise the singularity is to build a logarithmic representation of the amplitude of the maxima line versus scales. The mathematical formulation of this representation is given by Eq. (8), which introduces the Lipschitz exponent α. When the wavelet is the nth derivative of a gaussian, the maxima curves are connected and go through all of the finer scales. The decay rate of the maxima along the curves indicates the order of the isolated singularities [9].

$$\log_2(|Wf(u,s)|) \leqslant \log_2(A) + (\alpha + \tfrac{1}{2})\log_2(s). \tag{8}$$

More precisely, the Lipschitz exponent gives information about the differentiability of the function. The Lipschitz exponent is defined by: $n-1<\alpha<n$ (where n is the number of vanishing moments) and its value is inversely proportional to the size of the singularity. For example, if the value of exponent α is 1.5 at $x = x_0$, we know that this function is differentiable only once.

Another parameter, related to the relative magnitude of each singularity, can be extracted from Eq. (8): the intensity factor A.

2.3. Damage identification on displacement mode shape

The damage identification problem consists in locating and quantifying damaged zone(s). Wavelet transform offers the possibility to achieve these two levels of diagnosis as mode shapes contain local information about the local rigidity which is related to damage localisation and severity. Previous works [11] demonstrate the robustness of this method and the ability to distinguish damage from noise.

Following Hong et al. [3], we chose to study the first bending mode shape $Y_1(x)$, which can be decomposed in a smooth function $Y_{1\ \mathrm{smooth}}(x)$ and a singularity function $Y_{1\ \mathrm{Singular}}(x)$ as follows:

$$Y_1(x) = Y_{1\ \mathrm{smooth}}(x) + Y_{1\ \mathrm{Singular}}(x). \tag{9}$$

This last relation can be extended to any mode shapes. Generally, lowest frequency mode shapes are reliable.

It leads to characterise the singularity function by

$$|Y_{1\ \mathrm{Singular}}(x)| \leqslant K|x - x_V|^{\alpha}, \tag{10}$$

where K is the amplitude factor, x_v is the singularity location and α is the Lipschitz exponent. In practice $Y_{1\ \mathrm{smooth}}(x)$ is obtained from experimental data $Y_1(x)$ by fitting the analytical equation Eq. (4) using a nonlinear least-squares method. Then the function $Y_{1\ \mathrm{smooth}}(x)$ constitutes a baseline mode shape useful in the particular case of SHM approach based on no a priori information.

The Lipschitz exponent introduced above represents one of the principal parameters used to estimate the severity of a damage zone. Hong et al. [3] also conclude that to extract the Lipschitz exponent in the damaged beam problem using the wavelet transform the minimum number of the vanishing moments is $n = 2$. Based on these observations, Hong et al. [3] propose the mexican hat as a mother wavelet (corresponding to the second derivative of a Gaussian, $n = 2$) for detecting singularity on mode shape. For very small scales (1–4), the estimation of Lipschitz exponent is reliable and its value is included between $1<\alpha<2$ [12]. Douka et al [4] defined the intensity factor A which is easier to estimate than the Lipschitz exponent α and investigated the relation between wavelet transform coefficients and crack extent, described in terms of the intensity factor.

The local behaviour of these two severity indicators A and α has been studied form a parametric study. This numerical modal analysis is carried out by a finite element analysis software developed on Matlab using Euler–Bernouilli beam theory. Damage severity should vary from $\mathrm{d}I = 0.1$ (large damage) to $\mathrm{d}I = 0.9$ (small damage). The damage location should vary along the beam length for two BCs: clamped–clamped (CC) and clamped–free (CF). Damage size is constant (two-node beam element) for a sufficient number of elements to obtain good results ($N = 80$). The material data are $E = 206\,\mathrm{GPa}$, $\rho = 7850\,\mathrm{kg/m^3}$, and beam geometry is defined by $b = 0.032\,\mathrm{m}$, $h = 0.016\,\mathrm{m}$, $L = 0.72\,\mathrm{m}$.

Fig. 2. represents the behaviour of the 2 damage severity indicators for several damage location L_D/L for the clamped–clamped BCs. At each location, the Lipchitz exponent is inversly proportional to the damage severity. Fig. 2a. shows that α depends on the location of the damage zone L_D/L and so on the local curvature

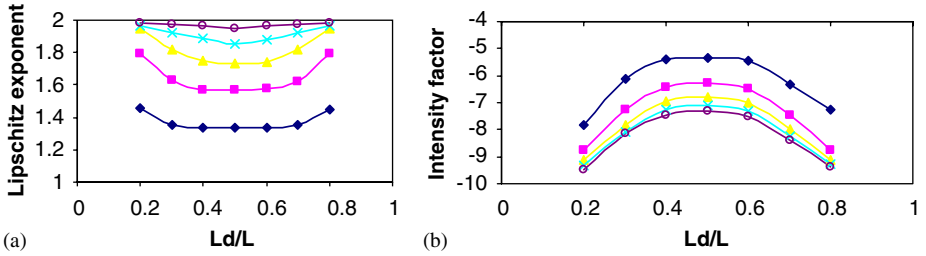

Fig. 2. Damage indicators behaviour (first bending mode) of the simulated beam for various locations L_D/L and variable severity dI: BCs = CC, Lipschitz exponent α (a) and intensity factor $\log_2(A)$ (b). Damage simulated by inertia reduction: ♦ d$I = 0.1$; ■ d$I = 0.3$; ▲ d$I = 0.5$; × d$I = 0.7$; *o* d$I = 0.9$.

of mode shape. Fig. 2b. exhibits also the impact of the curvature on the intensity factor A as expected from Refs. [3,4,10,11]. Finally it appears that the intensity of the parameters A and α is effectively correlated to the severity of the damage zone but their intensity depend also on the localisation of the damage zone and the BCs applied at beam ends.

3. Advanced damage identification method

Our advanced damage detection method (described in Fig. 3) can be divided into four successive steps:

- *Acquisition*: Modal parameters are obtained using an optimal sampling based on Sazonov and Klinkhachorn works [8]. This approach allows us to estimate high resolution mode shapes taking into account experimental noise and enables to evaluate even small damages. A pre-processing step consists in the exploitation of experimental mode shapes Y_i in order to obtain an estimation of mode shapes related to an undamaged state of the structure. This baseline state $Y_{i\text{smooth}}$ is produced using a fit between experimental values and the theoretical relation described in Eq. (3), according to classical hypothesis of material homogeneity and linear behaviour of structure.
- *Processing*: The processing step is based on the exploitation of mode shapes by CWT. Considering for example the first mode shape Y_1, the damaged zone can be located on the WSM by applying wavelet transform to Eqs. (9) and (10):

$$W_{Y_{1\text{Singular}}}(u,s) = \left| W_{Y_1}(u,s) - W_{Y_{1\text{smooth}}}(u,s) \right|. \tag{11}$$

  This equation is in good agreement with the theory, as $Y_{1\text{smooth}}(x)$ is a regular function; it means $W_{Y_{1\text{smooth}}}(u,s)$ is closed to zero at the singularity location. A Tuckey windowing function is applied to the mode shape in order to limit the boundary effects of the CWT computing. One of the advantages of this method is to limit noise effect on singularity detection.
- *Localisation*: Maxima lines are extracted from wavelet singular map and permit to estimate several significant indicators about the damage severity on both $W_{Y_1}(u,s)$ and WSM. Our estimation of Lipschitz exponent is slightly different from classical threshold methods which study the signal on scales (1:32) [3,4]. The advantage of WSM is to avoid threshold problems or nonlinearities of the maxima line along the scale range.
- *Identification*: The first step of the identification procedure is to estimate for each damage zone the Lipschitz exponent α and the intensity factor A directly on experimental data $W_{Y_1}(u,s)$ using the maxima lines obtained from WSM. Considering that α and A are only relative severity indicators our problem of identification is typically a pattern recognition problem which is often solved using a feed forward neural network with supervised learning. In order to improve the generalisation ability of neural network procedure we have introduced another severity indicator defined by $\text{SR} = \left|\alpha_M/A_M\right|$ (the absolute value of the ratio of Lipschitz exponent to intensity factor, obtained from the WSM). This indicator which is uncorrelated to α and A (due to the windowing and thresholding function applied on the WSM) vary slightly with damage location. The relevance of the damage indicator $\text{SR} = \left|\alpha_M/A_M\right|$ has been numerically

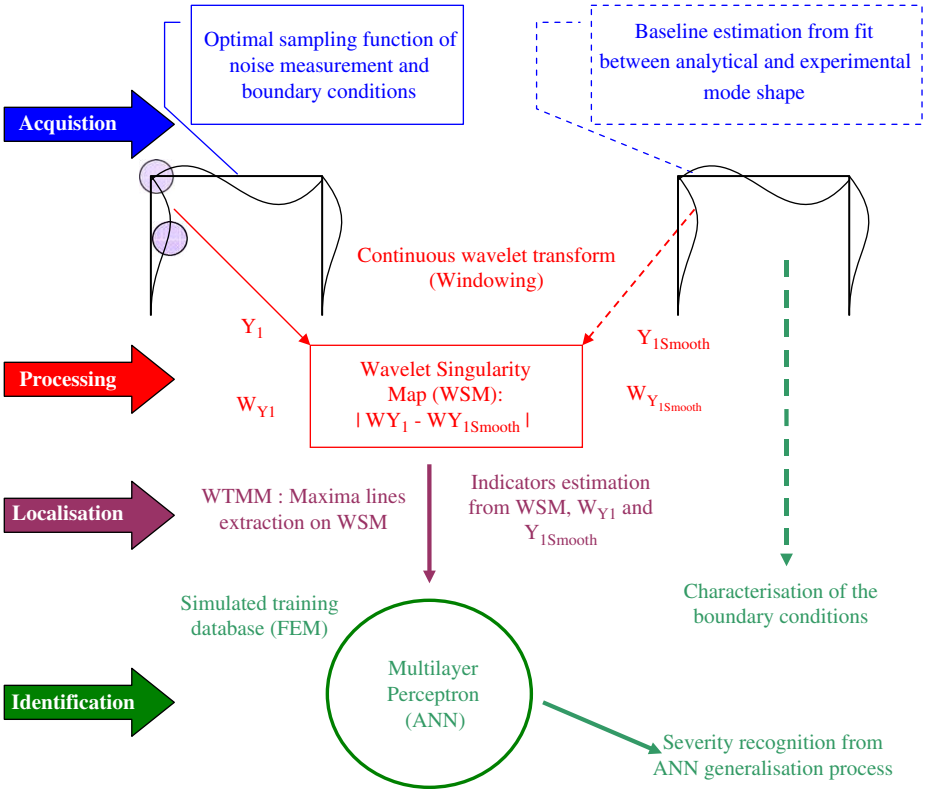

Fig. 3. Details of the advanced damage detection method including four steps: acquisition, processing, localisation and identification.

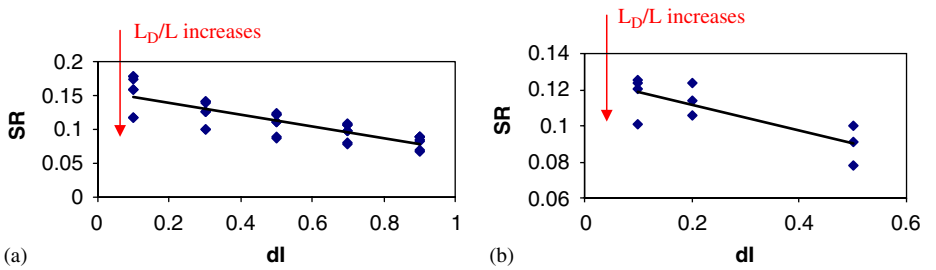

Fig. 4. Overall trend of our damage indicator SR (black line), which increases with the severity (dI decreases); each point ♦ associated with constant parameter dI is a function of damage location L_D/L which increases from top point to bottom point for the BCs = CC (a) and CF (b).

studied on the same beam used in Section 2.3 for two BCs, considering several locations and severities of the damage zone. In Fig. 4 the black line represents the overall trend of SR as a function of severity. For each location, SR is a decreasing function of dI; this means that the overall trend is a linear relationship with damage severity (for both BCs). It also illustrates that SR offers a range of variation which is less dependant on the damage location than α and A.

The neural network presented in Fig. 5 is trained to associate outputs with input patterns and then approximate any linear (or nonlinear) relationship between inputs and outputs. Practically, six input parameters are used: a global indicator of rigidity $\lambda_1 L$, two mode shape curvature indicators $\left|Y_1''(x = L_D)\right|$ and

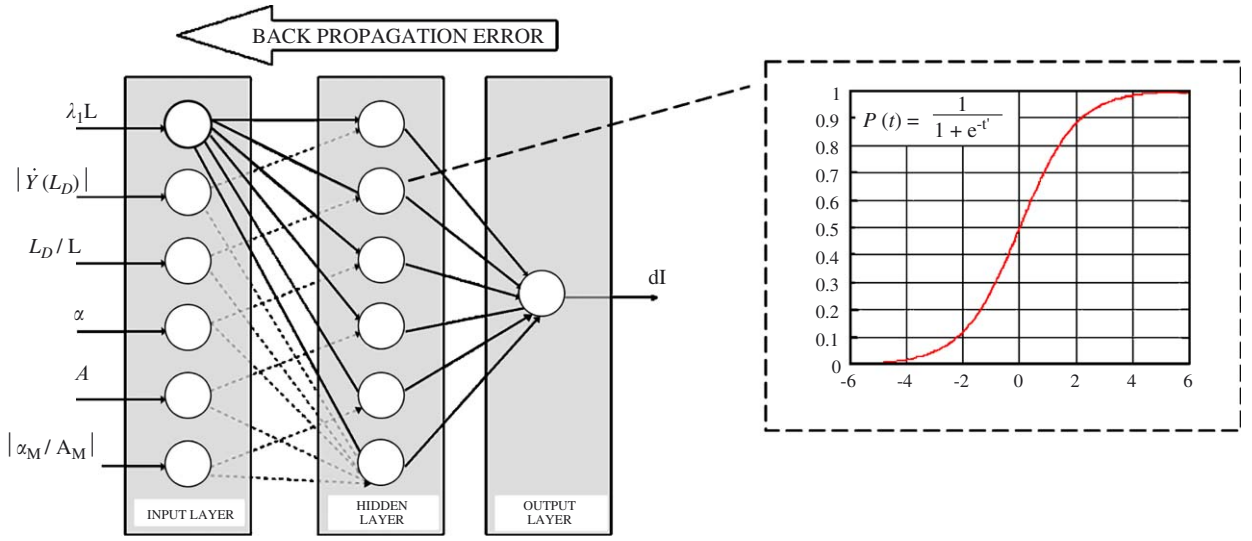

Fig. 5. Principle of the feed forward multilayer perceptron with sigmoid activation functions used to identify damage extent from the package of six extracted indicators.

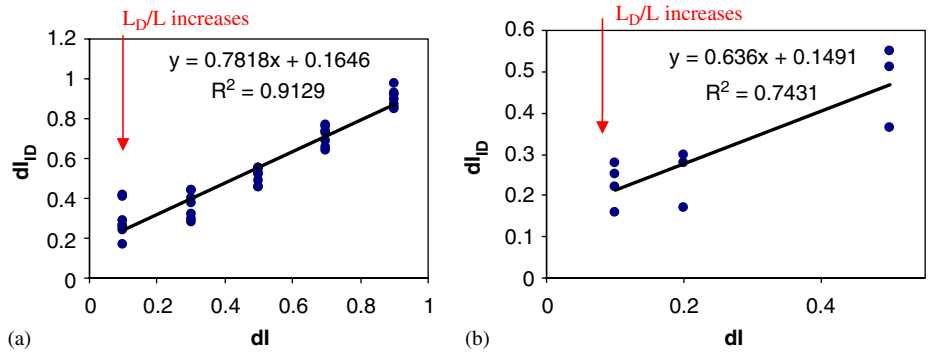

Fig. 6. Correlation between identified damage severity dI_{ID} and simulated damage extent dI: each point ● associated with constant parameter dI is a function of damage location L_D/L, which increases from top point to bottom point for BCs = CC (a) and CF (b).

L_D/L (where L_D is the damage location and L is the beam length), and three severity indicators α, A and $SR = |\alpha_M/A_M|$. This combination of six independant descriptors set is obtained by multiple tests on simulated data. More precisely, the recognition tool is designed with a multilayer perceptron (MLP) with two-layer feed forward and a hidden layer with six sigmoid functions, well adapted to recognition problems. A wide range of different damaged beams is computed (240 examples with different sizes of beam and different damage locations and severities) in order to set up an efficient training database. After learning using a Bayesian regularisation algorithm, the neural networks ouptut characterises the damaged zone by an identified inertia reduction factor dI_{ID} that corresponds to the experimental set of indicators (unlearned).

Finally we show in Fig. 6 some interesting numerical results with the NN classification: there is a good overall correlation (for all damage locations) between real damage extent dI and identified value dI_{ID}, with a correlation coefficient $R^2 > 0.91$ for CC and $R^2 > 0.74$ for CF. This phenomenon also enhances the curvature impact on the damage characterisation and the importance of finding the appropriate mode shape to analyse (in a complex structure). The correlation coefficient for cantilever beams is small, because damage is much more difficult to extract and because there are few CF simulations in the database.

4. Experimental results

The experimental setup consists in a Polytec PSV 400 scanning vibrometer for sensing and a shaker for excitation. In order to obtain experimental operating deflection shapes (ODS), we performed an acquisition to estimate the frequency response functions (FRFs) for all measurement points. The ODS were then calculated using an isolated frequency from the averaged FRF. At a given resonant frequency, if the ODS is dominated by one mode, then the ODS will closely approximate the mode shape, as the excitation force is not applied at a nodal line and the excitation sweeps around the resonance peak frequency.

In order to validate our numerical results, we conducted an experiment (Fig. 7b) on a timber portal frame. All the wood beams have the same section, $b \times h = 80 \times 80$ mm^2, and are 920 mm long. From all our data we extracted an interesting bending mode shape (the third portal frame resonance frequency at 264 Hz), as it clearly exhibits a large amplitude and a typical first bending mode shape for a beam with non perfect BCs. In fact, using structural dynamic response to locate small defects requires the use of high frequency deflection shapes with high curvature [14]. We focused on the double-damaged part of the portal (saw cuts in red in Fig. 7a). The first damage was inflicted at $L_{D1} = 487$ mm from the column base, with a depth of 13 mm and a width of 1.5 mm ($h = 67$ mm i.e. crack of 41% equivalent to $dI = 0.59$). The second damage (perpendicular to the first), 16 mm deep by 1.5 mm wide, was inflicted at $L_{D2} = 237$ mm from the clamped end ($b = 64$ mm i.e. crack of 20% equivalent to $dI = 0.8$).

- *Acquisition and processing*: The animated ODS was acquired using a 4×65 points map (Fig. 8) using optimal sampling resolution of 66 points/m following Sazonov's formulas [8] with $L = 0.9$ m (beam length) and $\varepsilon = 0.1\%$ (noise standard deviation from LDV). Then we extracted from the two-dimensional surface mode shape data the most probable mode shape, interpolated and averaged with the entire surface map, resulting in a vector of 260 points. This signal represents the medium line (overall) behaviour of the beam. The data are then fitted to analytical mode shape in Fig. 9:

$$y_{\text{fit}} = 0.255\ \cosh(3.719x) - 0.255\ \sinh(3.719x) - 0.175\ \cos(3.719x) + 0.869\ \sin(3.719x).$$

The first crack damage which belongs to the high-curvature part of the mode shape can be directly detected in Fig. 9. However, the second crack has much less effect as its variation of inertia is lower and as it lies within a low-curvature part of the signal. The WSM is then calculated (Fig. 10); it highlights three damaged zones and the heterogeneity of the material (small maxima lines around L_{D2}) as LDV noise standard deviation is classically low (close to 10^{-3}).

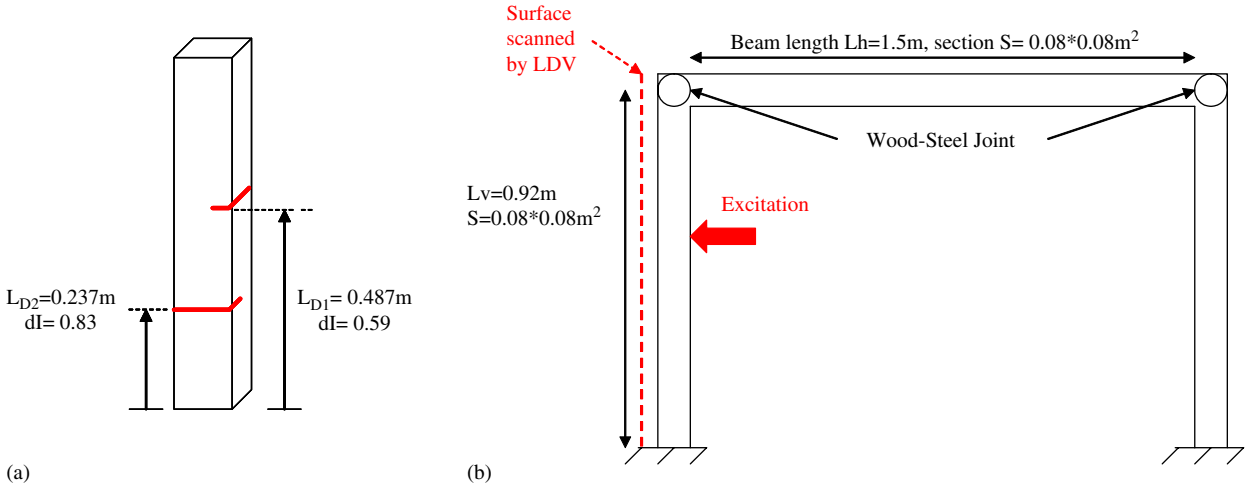

Fig. 7. Front view of the left-hand column under study with two damages at L_{D1} and L_{D2} (a) and schematic drawing of the portal frame with four wood-and-steel joints (b).

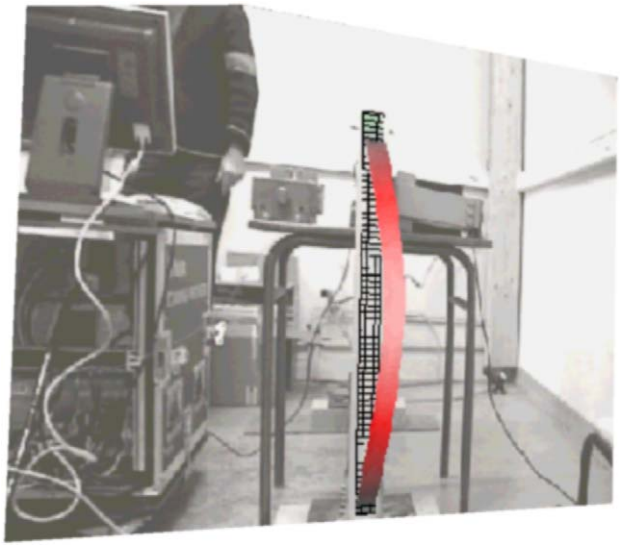

Fig. 8. Polytec software illustration of the animated bending ODS chosen at 264 Hz. The boundary conditions of the studied beam are clearly shown.

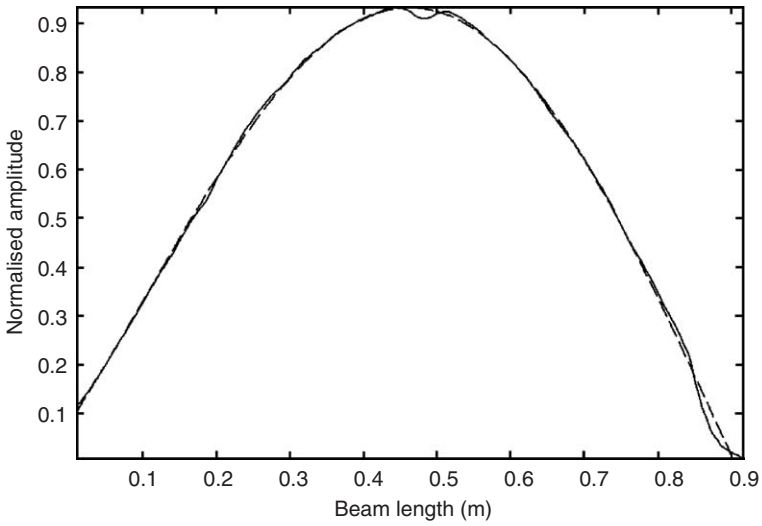

Fig. 9. Normalised experimental mode shape (bending mode at 264 Hz) extracted from the ODS (averaged and interpolated), which reveals the damages. —— Experimental data; – – – – fitted data.

- *Localisation and interpretation*: Fig. 10 leads to distinguish three singular parts. The first one corresponds to the damage zone located around $L = 0.2$ m. It represents a complex damage zone: the damage is well located and stands out clearly from noise (and heterogeneity) however some of its properties (maxima line slope) are very close to noise. Moreover, with a timber complex structure the problem of distinguishing damage from noise and the heterogeneity of the material remains. For this damage zone some parameters extracted from WSM are not included in the database range of our neural network. The step of identification cannot be realised for this damage zone. The second part represents the damage zone located at $L_{D1} = 0.487$ m. It clearly exhibits a strong maxima line in a high-curvature part of the mode shape. This damage zone will be analysed further. The third singular part

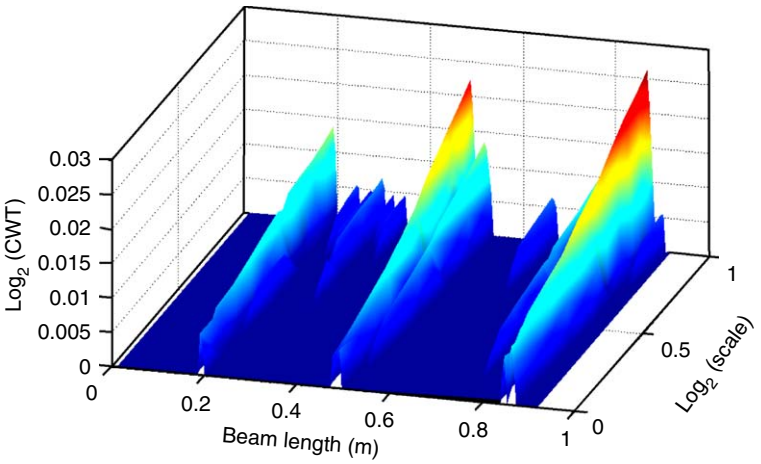

Fig. 10. Experimental wavelet singularity map (with threshold): joint time-scale representation of the experimental mode shape (scales are inversly proportionnal to frequency). Wavelet coefficients ($\log_2(CWT)$) are plotted versus $\log_2(scale)$ function of the mode shape (beam length L): the first two maxima lines represent the damages at L_{D1} and L_{D2} and the third line highlights the nonlinearity of the beam-to-column joint.

Table 1
Mode shape parameters and extracted indicators using the wavelet singularity map used to identify the damage severity for the damage at L_{D1}

Damaged mode shape parameters	Extracted indicators using WSM
$\lambda_1 L = 3.4215$	$\alpha = 1.36$
$\lvert Y' = (x = L_{D2})\rvert = 0.29$	$\log_2(A) = -7.61$
$L_D/L = 0.5311$	SR = 0.2

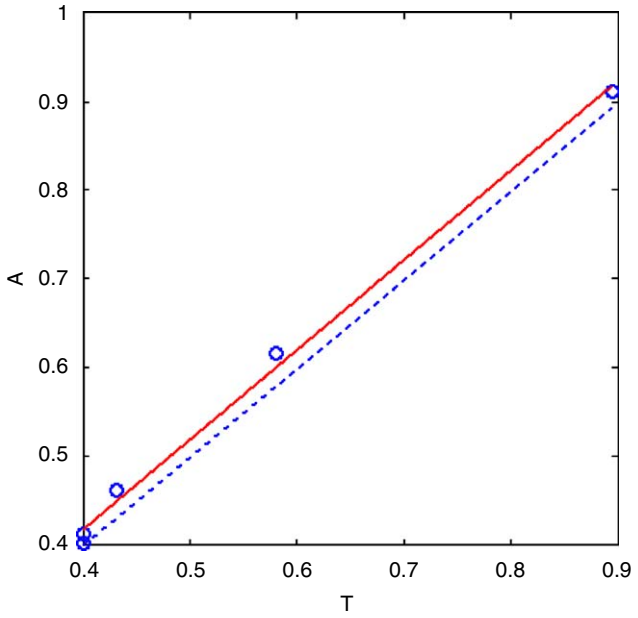

Fig. 11. Damage identification at L_{D1} (T are the NN targets and A the NN outputs) using optimal reduced database: severity $dI = 0.58$ identified at $dI_{ID} = 0.616$ with $R^2 = 0.996$ ($R = 0.998$). o Data points; —— best linear fit: $A = (1.01)\ T + (0.0148)$; – – – – $A = T$.

is correlated to the dissymmetry of mode shape representation (Fig. 9) observed on the extremities of the beam. The corresponding maxima line on WSM can be then interpreted as a high rigidity of the beam-to-column joint.

- *Identification*: The maxima line at L_{D1} is then extracted using our algorithm. It informs us about pertinent indicators (Table 1) which constituted the six inputs parameters of our damage extent recognition neural networks. Using these results we can identify $\mathrm{d}I_{\mathrm{ID}} = 0.616$ at L_{D1} with good confidence ($R^2 = 0.996$) in Fig. 11. Here we use a randomly chosen reduced database, generally more precise than the classical approach [10]. This robustness is explained if the extracted data are due to the same type of damage and beam dimensions. Its major drawback is the time it takes to converge to the optimal reduced database. For the BCs classification, the result $\pi \prec \lambda_1\ L = 3.4215 \prec 4.73$ indicates that the BCs are non-perfect; it represents the strong rigidity induced by the mortise-and-tenon joint (plus transverse steel rods) for the beam-to-column connection compared to the clamped base.

5. Conclusions

Our method is designed to establish the relation between pertinent damage indicators and damage severity using numerical examples. Wavelet transform can be used to locate the damage, while supervised neural networks are able to identify real damage using a simulated database. As an application we focused on a damaged part of a wooden portal frame. Using no a priori information, we succeeded in validating our method, locating structural damage very efficiently and identifying damage located on the high-curvature part of the mode shape. Further research should focus on a fuzzy expert system to automate the detection procedure in terms of its ability to properly distinguish damage from noise and heterogeneity. We also intend to qualify damage not only in term of inertia reduction but aslo in term of criticitity (probability of detection, false alarm). Finally the extracted features (including BCs characterisation) could be used to update a finite element model in order to validate an enhanced model update approach.

Acknowledgements

Particular thanks to Polytec France and especially J.-M. Laurent and for their active collaboration in data acquisition by scanning laser vibrometer.

References

[1] S.W. Doebling, C.R. Farrar, M.B. Prime, D.W. Shevitz, Damage identification and health monitoring of structural and mechanical systems from changes in their vibration characteristics: a literature review, Los Alamos National Laboratory Report LA—13070—MS.
[2] R.D. Adams, P. Cawley, The localisation of defects in structures from measurements of natural frequencies, *Journal of Strain Analysis* 14 (1979) 49–57.
[3] J.C. Hong, Y.Y. Kim, H.C. Lee, Y.W. Lee, Damage detection using the Lipschitz exponent estimated by the wavelet transform: applications to vibration modes of a beam, *International Journal of Solids and Structures* 39 (2002) 1803–1816.
[4] E. Douka, S. Loutridis, A. Trochidis, Crack identification in beams using wavelet analysis, *International Journal of Solids and Structures* 40 (2003) 3557–3569.
[5] A.B. Stanbridge, D.J. Ewins, Using a continuously scanning laser doppler vibrometer for modal testing, *Proceedings IMAC XIV*, 1996, pp. 816–822.
[6] S. Patsias, W.J. Staszewski, *Damage detection using optical measurements and wavelets*, Vol. 1, SHM, Sage Publications, Beverley Hills, CA, 2002 pp. 5–22.
[7] U.P. Poudel, G. Fu, J. Ye, Structural damage detection using digital video imaging technique and wavelet transformation, *Journal of Sound and Vibration* 286 (2005) 869–895.
[8] E. Sazonov, P. Klinkhachorn, Optimal spatial sampling interval for damage detection by curvature or strain energy mode shapes, *Journal of Sound and Vibration* 285 (2005) 783–801.
[9] S. Mallat, W.L. Hwang, Singularity detection and processing with wavelets, *IEEE Transactions on Information Theory* 38 (1992) 617–643.
[10] J. Morlier, F. Bos, P. Castera, Structural health monitoring of timber structure using advanced vibration analysis, Proceedings of fifth *International Conference on Acoustical and Vibratory Surveillance Methods and Diagnostic Techniques*, Senlis, France, October (2004).

[11] J. Morlier, F. Bos, P. Castera, Benchmark of damage localisation Algorithms using mode shape data, *Key Engineering Materials*, 293–294 (2005), pp. 305–312.
[12] J. Morlier, Méthodes d'Analyse des Déformées Modales pour le Diagnostic *in Situ* de Structures, Thèse de doctorat de l'Université de Bordeaux 1, 2005.
[13] N. Olgac, N. Jalili, Modal analysis of flexible beams with delayed resonator vibration absorber: Theory and experiments, *Journal of Sound and Vibration* 218 (1998) 307–331.
[14] P. Frank Pai, L. Huang, S.H. Gopalakrishnamurthy, J.H. Chung, Identification and applications of boundary effects in beams, *International Journal of Solids and Structures* 41 (2004) 3053–3080.
[15] J. McGuire, *Notes on semi-rigid connections*, FEMCI book, NASA, USA, 1995.
[16] A.K. Pandey, M. Biswas, M.M. Samman, Damage detection from changes in curvature mode shapes, *Journal of Sound and Vibration* 145 (1991) 321–332.